Available online at www.sciencedirect.com

SciVerse ScienceDirect

Ceramics International 38 (2012) 1649–1654

CERAMICS INTERNATIONAL

www.elsevier.com/locate/ceramint

Hydrothermal synthesis of porous hydroxyapatite ceramics composed of rod-shaped particles and evaluation of their fracture behavior

Setsuaki Murakami [a], Katsuya Kato [a], Yuki Enari [b], Masanobu Kamitakahara [b], Noriaki Watanabe [b], Koji Ioku [b,*]

[a] National Institute of Advanced Industrial Science and Technology (AIST), 2266-98 Anagahora Shimoshidami Moriyama-ku, Nagoya 463-8560, Japan
[b] Graduate School of Environmental Studies, Tohoku University, 6-6-20 Aoba, Aramaki, Aoba-ku, Sendai 980-8579, Japan

Received 7 May 2011; received in revised form 25 September 2011; accepted 28 September 2011
Available online 5 October 2011

Abstract

We previously reported that porous hydroxyapatite (HA) ceramics composed of rod-shaped particles exhibited high functional ability to be integrated in natural bone quickly compared to sintered HA ceramics. In addition to improved biological properties, rod-shaped particles might also provide unique mechanical properties to the HA porous ceramics. In this study, porous HA ceramics composed of rod-shaped HA particles with different aspect ratios were synthesized by a hydrothermal process, and their fracture behavior was examined by a flexural test. As the reaction temperature in the hydrothermal process decreased, the aspect ratio of the resultant particles increased and was successfully controlled from 13 to 37. Porous HA ceramics composed of rod-shaped particles with large aspect ratios exhibited non-elastic deformation in the flexural test. As the aspect ratio of the particles increased, the flexural strength and strain at fracture increased. Furthermore, the flexural strength and strain at fracture of the porous HA ceramics composed of rod-shaped particles with large aspect ratios was higher than that of sintered porous HA ceramics with a similar porosity.

Keywords: C. Mechanical properties; D. Apatite; E. Biomedical applications

1. Introduction

Hydroxyapatite ($Ca_{10}(PO_4)_6(OH)_2$; HA) is a major component of human hard tissue, such as bones and teeth. HA ceramics have been used as a bone-repairing material because they can bond directly to natural bones [1,2]. Porosity, microstructure and mechanical properties are important attributes for HA ceramics intended for use as artificial bones. An artificial bone with high porosity would be suitable for bone regeneration due to the infiltration of tissue into the pores of the material, but the strength of artificial bone decreases markedly with increased porosity [3]. Moderate mechanical strength is necessary for HA ceramics because with insufficient strength, the material lacks workability. Therefore, an artificial bone with high porosity and moderate strength is required, although the exact properties required depend on the part of body intended for the implant. Attempts to reinforce the strength and fracture toughness of ceramics by the addition of fiber to HA matrix ceramics have been reported [4–6]. It is expected that such reinforcement can be achieved by HA particles themselves if the HA ceramics are constructed from fiber-shaped or rod-shaped HA particles.

We previously synthesized porous HA materials composed of rod-shaped particles with controlled porosity through a hydrothermal process [7–10], and these materials showed some advantages over sintered porous HA ceramics composed of globular particles. Porous HA ceramics composed of rod-shaped particles adsorbed an acidic protein selectively [11]. When the porous HA ceramics composed of rod-shaped particles were implanted in bone defects in rabbit femurs, the implanted porous HA ceramics were integrated in natural bone quickly and exhibited bioresorbability [12]. In addition to these physicochemical and biological properties, the microstructures constructed by the rod-shaped particles are useful in trapping certain functional particles within the pores by the tangling of the rod-shaped particles, providing the composite materials with new functionalities [13,14].

* Corresponding author. Tel.: +81 22 795 7407; fax: +81 22 795 7407.
E-mail address: ioku@mail.kankyo.tohoku.ac.jp (K. Ioku).

0272-8842/$36.00
doi:10.1016/j.ceramint.2011.09.056

It is expected that porous HA ceramics composed of rod-shaped particles might also have some advantages in mechanical properties. In a ceramic composed of rod-shaped particles, the aspect ratio of the particles is expected to influence the mechanical properties significantly. We previously reported the compressive strength of porous HA ceramics composed of rod-shaped particles and their unique fracture behavior [15], but the effect of the aspect ratio was not discussed. In the present study, porous HA ceramics with high porosities (about 60%) composed of rod-shaped particles with different aspect ratios were prepared by a hydrothermal process. The fracture behavior of the porous HA ceramics composed of rod-shaped particles was evaluated by a flexural test, and the effect of the aspect ratio of rod-shaped particles on the mechanical properties is discussed.

2. Experimental method

2.1. Preparation of porous HA

A powdered 2 g sample of α-tricalcium phosphate ($Ca_3(PO_4)_2$, α-TCP; Taihei Chemical Industrial Co., Ltd., Japan) was molded in a stainless steel die (15 mm × 40 mm) under a compressive pressure of about 1 MPa with the addition of 0.4 cm^3 of distilled water. After the molding, four rectangular specimens (about 15 mm × 40 mm × 3 mm) were set in each 350 cm^3 autoclaves with 120 cm^3 of distilled water and exposed to water vapor under saturated vapor pressure at 105 °C, 160 °C and 240 °C for 24 h, respectively. A schematic illustration of the process is shown in Fig. 1. The specimens were then retreated hydrothermally at 105 °C for 3 h in an ammonia solution at pH 11 under immersion conditions to complete the reaction from α-TCP to HA. After the hydrothermal treatments, the specimens were dried at 90 °C in air. The samples were named HHA105, HHA160 and HHA240, respectively, derived from the temperatures of the initial hydrothermal treatment.

For comparison, sintered HA porous ceramics (SHA) were also prepared. Hydroxyapatite powder (HA $Ca_{10}(PO_4)_6(OH)_2$; Ube Material Ind., Japan) was used as the starting material. The HA powder (2 g) was molded in a stainless steel die (15 mm × 40 mm) under a compressive pressure of about 1 MPa with the addition of 0.4 cm^3 of water. After molding, the rectangular specimens (about 15 mm × 40 mm × 4 mm) were sintered at 1000 °C in air for 24 h.

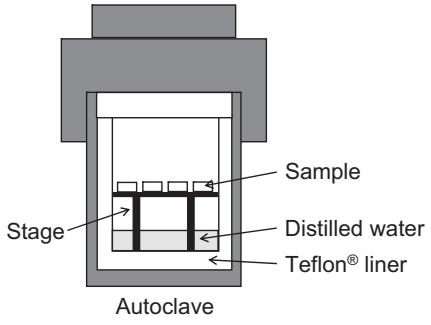

Fig. 1. Schematic illustration of hydrothermal treatment with water vapor.

2.2. Evaluation of structures and fracture behavior

The crystal phases of the specimens were identified by powder X-ray diffractometry with a CuKα radiation, operating at 40 kV and 30 mA (XRD; RINT-2100VL, Rigaku Co., Japan).

The particle morphology was observed using field emission scanning electron microscopy (FE-SEM, S-4300, Hitachi, Japan). For the SEM experiments, a thin coating of Pt was deposited on the surface of the product. Aspect ratios (*c*-axis length/*a*-axis length) of rod-shaped HA particles were determined from SEM photographs. Fifty particles whose appearance could be observed were selected in the SEM photograph, and their *c*-axis length, *a*-axis length and aspect ratio (*c*-axis length/*a*-axis length) were obtained.

The porosity (p) of the specimens was calculated by the bulk density (ρ_b) of the specimens and the theoretical density (ρ_t) of HA (3.16 g cm^{-3}) [16]. The bulk density (ρ_b) was calculated by dry weight and the volume of the specimen. Eq. (1) shows the formula for calculating the porosity (p) of the specimens.

$$p = \left(\frac{1-\rho_b}{\rho_t}\right) \times 100 \quad (1)$$

Eight specimens for each sample were examined, and the average value was obtained.

Rectangular specimens were used to measure the three-point flexural strength. The tests were conducted in a strength testing machine (Model EZ Graph, Shimadzu, Japan). The flexural strength and the strain were calculated by the following equations,

$$\text{Flexural strength}: \quad \sigma_{b3} = \frac{3PL}{2wt^2} \quad (2)$$

$$\text{Strain}: \quad \varepsilon = \frac{6t\Delta l}{L^2} \quad (3)$$

where σ_{b3} is the flexural strength in MPa, P is the maximum load in N, L is the fulcrum distance in mm, w is the width of the specimen in mm, t is the thickness of the specimen in mm and Δl is the deflection in mm.

A crosshead speed was 0.1 mm min^{-1}, and the fulcrum distance was 20 mm. Eight specimens for each sample were examined, and the average value was obtained.

3. Results

XRD patterns of samples of HHA105, HHA160, HHA240 and SHA are shown in Fig. 2. After hydrothermal treatments, α-TCP was completely changed into HA. As the reaction temperature increased, the diffraction lines ascribed to HA became sharper.

SEM micrographs of surfaces of the samples of HHA105, HHA160, HHA240 and SHA are shown in Fig. 3. All of the samples prepared by hydrothermal treatments were mainly composed of rod-shaped HA particles elongated along the *c*-axis. Changes in *a*-axis length, *c*-axis length and the aspect ratio (*c*-axis length/*a*-axis length) of the rod-shaped HA particles prepared at the different reaction temperatures are shown in

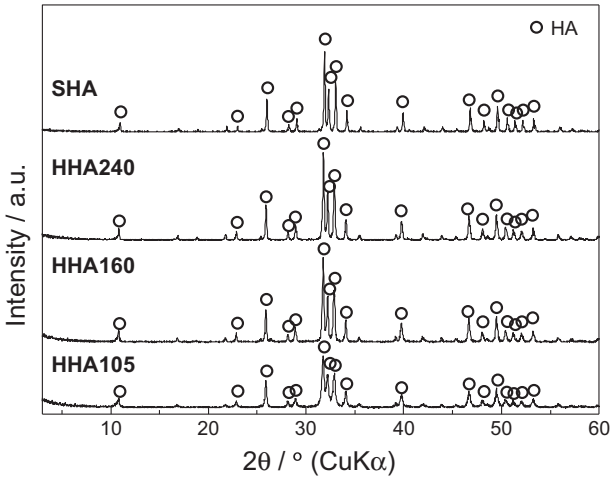

Fig. 2. XRD patterns of HHA105, HHA160, HHA240 and SHA.

Fig. 4. The *a*-axis length of rod-shaped HA particles increased with increasing reaction temperature. The *c*-axis length of the rod-shaped HA particles decreased with increasing reaction temperature. Consequently, the aspect ratio of rod-shaped HA particles decreased with increasing reaction temperature. In contrast, the sintered porous HA ceramic was composed of globular particles, and the neck between the globular particles due to sintering was observed.

The porosities of all porous HA ceramics prepared by the hydrothermal treatment were about 63% despite the different hydrothermal conditions, and the porosities of the porous HA ceramics prepared by the sintering method were about 60%.

To investigate the mechanical properties of the porous HA ceramics composed of rod-shaped particles with different aspect ratios, three point flexural tests were performed. Fig. 5 shows representative stress–strain curves for HHA105 and SHA. When a load was applied on the sintered ceramic (SHA), stress increased with strain, and the material showed brittle failure. However, the strain of the porous HA ceramic composed of rod-shaped particles with a large aspect ratio (HHA105) increased up to about 1.0% non-monotonically, much larger than the increase for SHA. The larger area under the stress–strain curve of HHA105 indicates that HHA105 is more difficult to fracture than SHA. The stress–strain curve of HHA105 seems to be divided into two regions (regions 1 and 2). In region 1, the stress increased very little with increasing strain, while the stress increased linearly in region 2. At a strain of about 1.0%, HHA105 was fractured.

Fig. 6 shows SEM micrographs of (a) the surface when the load was applied by the crosshead before fracture (region 1) and (b) the fractured surface of HHA105. The imprint of the crosshead was observed due to the rearrangement of the rod-shaped HA particles on the surface before fracture. Rod-shaped particles were also observed in the fractured surface of HHA105.

Fig. 7 shows the relationship between the strain and the aspect ratio of the rod-shaped particles that compose the porous HA ceramics. Fig. 8 shows the relationship between the flexural strength of the porous HA ceramics and the aspect ratio of the rod-shaped particles. As the aspect ratio increased, both the strain at fracture and the flexural strength increased. When the aspect ratio was 37 (HHA105), the strain at fracture and the flexural strength were the highest observed for the HA ceramics with rod-shaped particles and were higher than those of SHA with similar porosity.

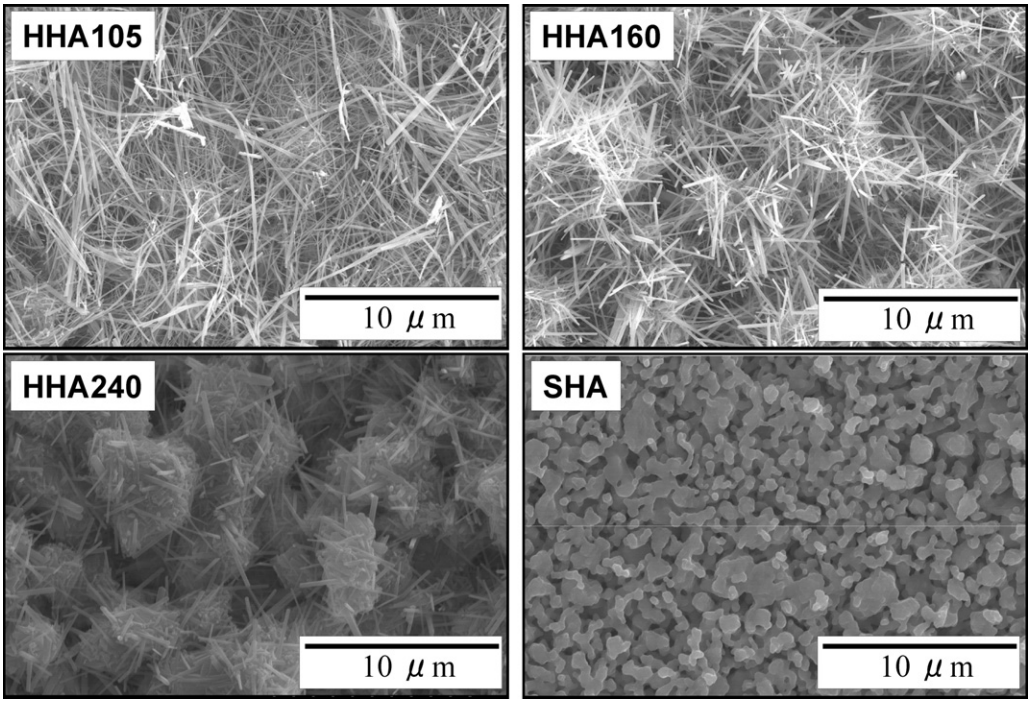

Fig. 3. SEM micrographs of the surfaces of samples HHA105, HHA160, HHA240 and SHA.

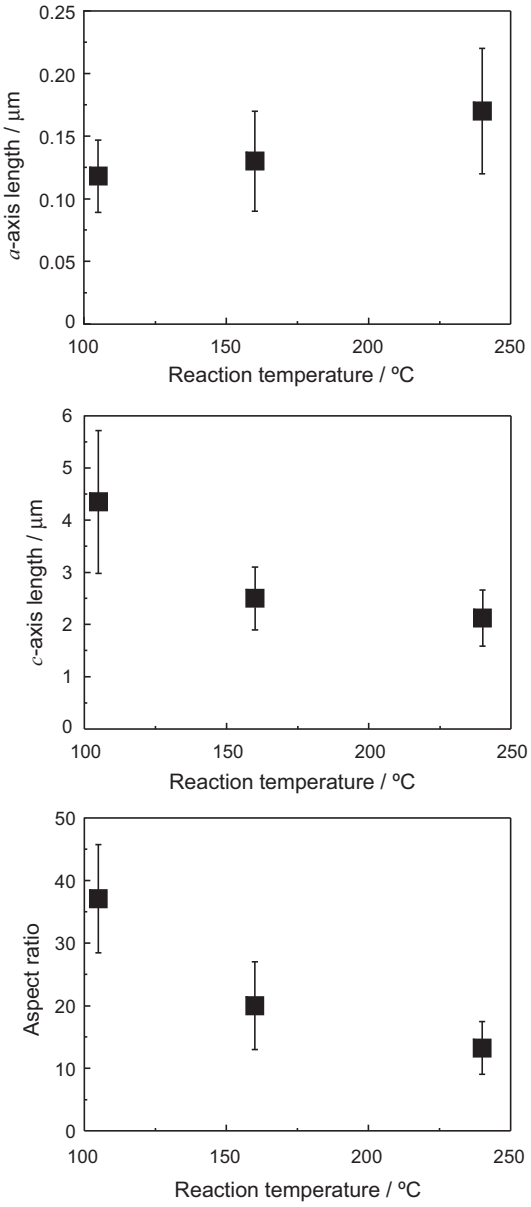

Fig. 4. Reaction temperature dependence of *a*-axis length, *c*-axis length and the aspect ratio of rod-shaped HA particles prepared by hydrothermal treatments.

4. Discussion

When porous α-TCP ceramics were treated hydrothermally, they changed into porous HA ceramics and consequently hardened [17]. The reaction between α-TCP and water is considered as follows, assuming that the HA obtained was stoichiometric HA.

$$10\alpha\text{-}Ca_3(PO_4)_2 + 6H_2O \rightarrow 3Ca_{10}(PO_4)_6(OH)_2 + 2H_3PO_4$$

In the hydrothermal treatments under water vapor, the phosphoric acid formed did not diffuse easily in the reaction solutions. Therefore, the specimens were retreated hydrothermally at 105 °C for 3 h in an ammonia solution (pH 11) to complete the reaction from α-TCP to HA. After hydrothermal treatment, the reaction from α-TCP to HA was complete, and

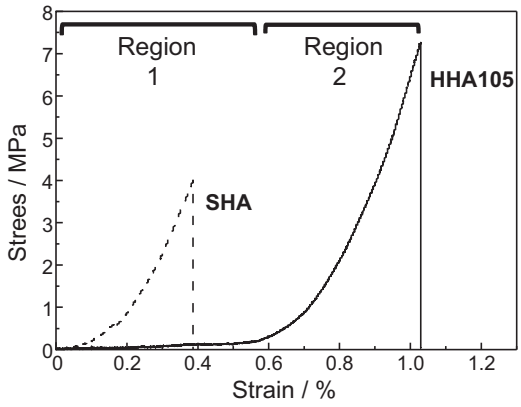

Fig. 5. Representative stress–strain curve of HHA105. The dotted line indicates the stress–strain curve of the SHA sample.

the phase observed by XRD for all of the specimens was HA (Fig. 2).

The surface of all specimens was mainly composed of rod-shaped HA particles elongated along the *c*-axis and had submicron-sized pores formed through the tangling of rod-shaped particles. The rod-shaped particles were elongated along the *c*-axis at lower reaction temperatures. As the reaction temperature increased, the *a*-axis length of rod-shaped particles increased, and the *c*-axis length decreased. Suzuki et al. reported that surface energies on rod-shaped particles of $Sr_5(PO_4)_3Cl$ and $Ba_5(PO_4)_3Cl$, which have apatite structures, were dependent on their faces, and the materials tended to elongate in the ⟨0 0 0 1⟩ direction [18]. Therefore, crystal growth of HA should also be dependent on the surface energy anisotropy, and HA crystals would easily be elongated along the *c*-axis.

Yoshimura et al. reported that when a HA slurry of a $Ca(OH)_2$–H_3PO_4 system was treated hydrothermally in acid or alkali solutions, rod-shaped HA particles were elongated along the *c*-axis in acid solutions, while rod-shaped particles were not elongated along the *c*-axis in alkali solutions [19]. In our study, HA and phosphoric acid were formed by the reaction of α-TCP and water. It is speculated that the *a*-face of rod-shaped particles was dissolved by phosphoric acid, and the *c*-axis length was increased by crystal growth on the *c*-face. The reaction from α-TCP to HA proceeded through the dissolution and subsequent precipitation at different crystal faces. At low reaction temperatures, the rod-shaped particles were elongated along the *c*-axis. However, at high reaction temperatures, the rod-shaped particles were not elongated along the *c*-axis because the reaction rate was significantly increased and the reaction finished within a short time.

When loads were applied to the specimens, SHA fractured easily. However, porous HA ceramics composed of rod-shaped particles with large aspect ratios (HHA105) showed larger deformation before fracture. The rod-shaped particles may prevent the propagation of the crack. In region 1 in Fig. 5, porous HA ceramics composed of rod-shaped particles could be deformed without fracture. This deformation occurred by the rearrangement of rod-shaped particles by the load. Fig. 6(a)

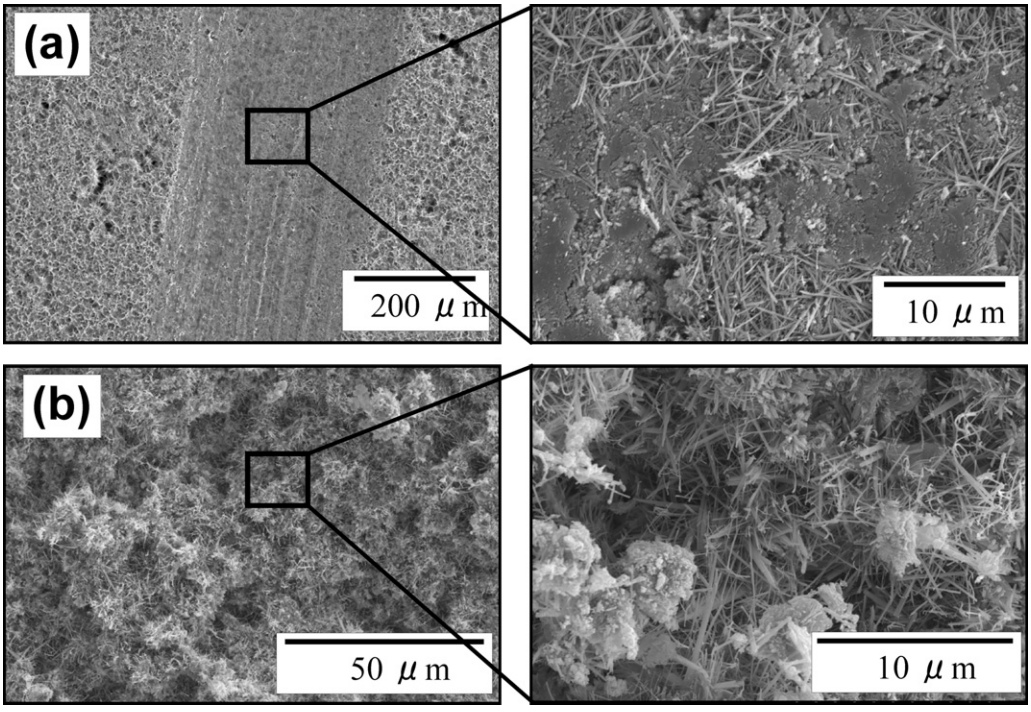

Fig. 6. SEM micrographs of (a) the surface when the load was applied by the crosshead before fracture and (b) the fractured surface of HHA105.

shows that the surface was deformed by the loading of the crosshead. In region 2, elastic deformation of rod-shaped particles themselves and loosening of the tangled particles occurred.

As the aspect ratio increased, the strain of the porous HA ceramics increased. Consequently, the flexural strength of the porous HA ceramics increased. The high flexural strength is explained by the tangling of rod-shaped particles. As rod-shaped particles were elongated along the *c*-axis, the contact point of the rod-shaped particles increased. Although the porosities of the porous HA ceramics were nearly the same, the flexural strength of HHA105 composed of rod-shaped particles with an aspect ratio of 37 was highest in the HA ceramics with rod-shaped particles and was higher than that of the SHA ceramic because the applied stress was dispersed by the rod-shaped particles. The high aspect ratio of rod-shaped particles reinforced the mechanical strength of the porous HA ceramic.

The porous HA ceramics composed of rod-shaped particles with a large aspect ratio are suitable for use as artificial bones with respect to the mechanical properties for handling. Previously, implanted porous HA ceramics composed of rod-shaped particles were integrated in natural bone quickly and showed bioresorbability [12]. These results indicate that HA ceramics composed of rod-shaped particles are promising for use as artificial bone. The aspect ratio of rod-shaped HA particles may also affect the biological properties, and this will be evaluated in future work.

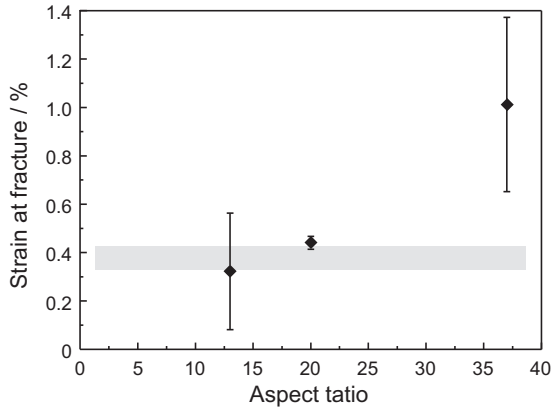

Fig. 7. Relationship between the strain at fracture of the HA porous ceramics and the aspect ratio of HA particles that compose the porous HA ceramics. The gray area indicates the strain at fracture of SHA, including the standard deviation.

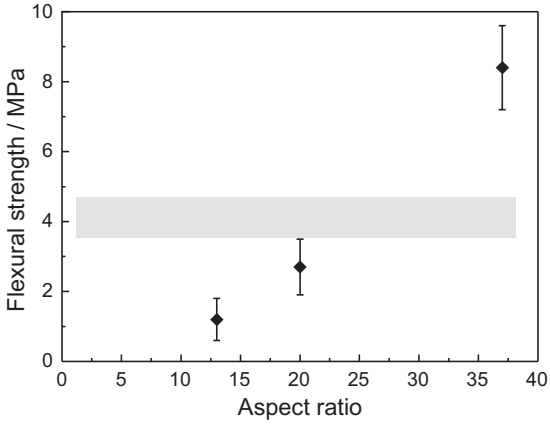

Fig. 8. Relationship between the flexural strength of porous HA ceramics and the aspect ratio of HA particles that compose the porous HA ceramics. The gray area indicates the flexural strength of SHA, including the standard deviation.

5. Conclusion

Porous HA ceramics composed of rod-shaped particles with different aspect ratios were prepared by varying the hydrothermal reaction temperature. As the aspect ratio increased, the flexural strength and strain at fracture of porous HA ceramics increased. Porous HA ceramics composed of rod-shaped particles with large aspect ratios would be useful as novel bone-repairing ceramics which show high mechanical strength and are not fragile.

Acknowledgements

This research was partially supported by JSPS KAKENHI 21300175. The authors thank Profs. K. Tohji and E.H. Ishida of Tohoku University for their honest support for measurement.

References

[1] L.L. Hench, Bioceramics: from concept to clinic, J. Am. Ceram. Soc. 74 (1991) 1487–1510.
[2] R.Z. LeGeros, Properties of osteoconductive biomaterials: calcium phosphates, Clin. Orthop. Relat. Res. 395 (2002) 81–98.
[3] Y. Zhang, Y. Yokogawa, X. Feng, Y. Tao, Y. Li, Preparation and properties of bimodal porous apatite ceramics through slip casting using different hydroxyapatite powders, Ceram. Int. 36 (2010) 107–113.
[4] Y. Zhang, S. Tan, Y. Yin, C-fibre reinforced hydroxyapatite bioceramics, Ceram. Int. 29 (2003) 113–116.
[5] A. Slosarczyk, M. Klisch, M. Blazewicz, J. Piekarczyk, L. Stobierski, A. Rapacz-Kmita, Hot pressed hydroxyapatite–carbon fibre composites, J. Eur. Ceram. Soc. 20 (2000) 1397–1402.
[6] S. Kobayashi, W. Kawai, Development of carbon nanofiber reinforced hydroxyapatite with enhanced mechanical properties, Composites Part A 38 (2007) 114–123.
[7] K. Ioku, Y. Eguchi, H. Fujimori, S. Goto, W. Suchanek, M. Yoshimura, Porous materials of calcium hydroxyapatite and strontium hydroxyapatite prepared hydrothermally, Phosphorus Res. Bull. 9 (1999) 11–16.
[8] K. Ioku, G. Kawachi, S. Sasaki, H. Fujimori, S. Goto, Hydrothermal preparation of tailored hydroxyapatite, J. Mater. Sci. 41 (2006) 1341–1344.
[9] K. Ioku, G. Kawachi, N. Yamasaki, M. Toda, H. Fujimori, S. Goto, Hydrothermal preparation of porous hydroxyapatite with tailored crystal surface, Key Eng. Mater. 288–289 (2005) 521–524.
[10] M. Kamitakahara, C. Ohtsuki, G. Kawachi, D. Wang, K. Ioku, Preparation of hydroxyapatite porous ceramics with different porous structures using a hydrothermal treatment with different aqueous solutions, J. Ceram. Soc. Jpn. 116 (2008) 6–9.
[11] T. Takahashi, M. Kamitakahara, G. Kawachi, K. Ioku, Preparation of spherical porous granules composed of rod-shaped hydroxyapatite and evaluation of their protein adsorption properties, Key Eng. Mater. 361–363 (2008) 83–86.
[12] T. Okuda, K. Ioku, I. Yonezawa, H. Minagi, Y. Gonda, G. Kawachi, M. Kamitakahara, Y. Shibata, H. Murayama, H. Kurosawa, T. Ikeda, The slow resorption with replacement by bone of a hydrothermally synthesized pure calcium-deficient hydroxyapatite, Biomaterials 29 (2008) 2719–2728.
[13] S. Murakami, T. Hosono, B. Jeyadevan, M. Kamitakahara, K. Ioku, Hydrothermal synthesis of magnetite/hydroxyapatite composite material for hyperthermia therapy for bone cancer, J. Ceram. Soc. Jpn. 116 (2008) 950–954.
[14] S. Ji, S. Murakami, M. Kamitakahara, K. Ioku, Fabrication of titania/hydroxyapatite composite granules for photo-catalyst, Mater. Res. Bull. 44 (2009) 768–774.
[15] K. Ioku, M. Toda, S. Sasaki, H. Fujimori, S. Goto, Preparation of functional apatite by controlling crystal surface, Jpn. J. Clin. Biomech. 25 (2004) 63–68.
[16] V.S. Komlev, S.M. Barinov, Hydroxyapatite and hydroxyapatite-based ceramics, Inorg. Mater. 38 (2002) 1159–1172.
[17] H. Monma, Preparation of octacalcium phosphate by the hydrolysis of α-tricalcium phosphate, J. Mater. Sci. 15 (1980) 2428–2434.
[18] T. Suzuki, G. Hirose, S. Oishi, Contact angle of water droplet on apatite single crystals, Mater. Res. Bull. 39 (2004) 103–108.
[19] M. Yoshimura, H. Suda, K. Okamoto, K. Ioku, Hydrothermal synthesis of needle-like apatite crystal, Nippon Kagaku Kaishi 10 (1991) 1402–1407 (in Japanese).